

# The role of energetic electrons on non-inductive current start-up and formation of an inboard poloidal field null configuration in the spherical tokamak QUEST

S. TASHIMA<sup>1</sup>, H. ZUSHI<sup>2</sup>, M. ISOBE<sup>3</sup>, H. IDEI<sup>2</sup>, S. OKAMURA<sup>3</sup>, K. HANADA<sup>2</sup>, K. NAKAMURA<sup>2</sup>, A. FUJISAWA<sup>2</sup>, K. MATSUOKA<sup>2</sup>, M. HASEGAWA<sup>2</sup>, Y. NAGASHIMA<sup>2</sup>, M. ISHIGURO<sup>1</sup>, S. KAWASAKI<sup>2</sup>, H. NAKASHIMA<sup>2</sup>, A. HIGASHIJIMA<sup>2</sup>

<sup>1</sup>*IGSES, Kyushu University, Kasuga, Fukuoka, 816-8580, Japan*

<sup>2</sup>*RIAM, Kyushu University, Kasuga, Fukuoka, 816-8580, Japan*

<sup>3</sup>*National Institute for Fusion Science, 509-5292, Toki, Japan*

## 1. INTRODUCTION

Non-inductive current start up and sustainment using electron cyclotron resonance heating (ECH), aiming at steady state operation of the fusion tokamak, has been studied on the several devices [1 - 5]. In the current start-up phase, three mechanisms for initial current  $I_p^{\text{initial}}$  have been proposed as follows; the pressure-driven current  $j_{pd}$  [6], co-moving electrons characterized by stagnation orbits  $j_{co}$ [7,8], and toroidal precession of trapped electrons  $j_{pr}$ . Since the direction of these currents depends on the sign of the vertical field  $B_z$ , the effect of curvature and the magnitude of  $B_z$  or mirror ratio  $R_{\text{mirror}}$  of the toroidal field  $B_t$  on  $I_p^{\text{initial}}$  is studied to verify the dominant mechanism or evaluate the fraction of mechanisms. Here,  $R_{\text{mirror}}$  is defined as the ratio of  $B_t$  at the wall and  $B_t$  at the mid plane along the field lines. In the steady state phase, the fraction of  $B_z/B_t$  on  $I_p$  and equilibrium is also investigated. High beta poloidal  $\beta_p$  equilibrium with an inboard null is found at high  $B_z/B_t$  and high  $R_{\text{mirror}}$ . The role of the energetic electrons created by ECH on  $I_p^{\text{initial}}$ , and formation and sustainment of high poloidal beta  $\beta_p$  plasma is studied with measurement of hard X-rays (HXR).

## 2. EXPERIMENTAL SETUP

QUEST is a medium sized device, whose inner and outer diameters are 0.2 m and 1.4 m, respectively. Two flat divertor plates are set at  $Z = \pm 1$  m from the mid-plane. The major ( $R_0$ ) and minor ( $\langle a \rangle$ ) radii of the plasma are 0.7 – 0.85 m and 0.2 – 0.4 m, respectively. RF waves at the frequency of 8.2 GHz are used to initiate plasma.  $B_t$  is 0.29 T and the fundamental resonance locates at  $R_{\text{res1}} = 0.3$  m. The typical plasma density  $n_e$  is below the cut-off density  $n_{\text{cut}}$  ( $\sim 8.6 \times 10^{17} \text{ m}^{-3}$ ). Since the chamber aspect ratio is 1.33 and 1<sup>st</sup> -3<sup>rd</sup> harmonics co-exist, electrons can interact with ECWs at various parallel refractive indices  $N_{\parallel}$ . Up to 50 kW of rf power is injected in the O-mode at  $N_{\parallel 0} < 0.4$ . The  $R_{\text{mirror}}$  is varied from 0.85 to 2 by choosing

three pairs of poloidal field coils. For  $R_{\text{mirror}} < 1$ , the magnetic field lines are convex indicating the negative curvature. The ratio of  $B_z/B_t$  is varied up to 10 % at  $2 \times R_{\text{res}1}$ . The semiconductor detector CdTe, whose size is  $3 \times 3 \times 1 \text{ mm}^3$ , is used to detect bremsstrahlung emitted by energetic electrons in the energy range  $< 1 \text{ MeV}$ . Pulse height analysis is used to obtain the energy spectrum with a time resolution of a few msec. The observation lines view plasma tangentially on the mid plane with the radial resolution of  $\pm 0.1 \text{ m}$  at  $R_{\text{tan}}$  of  $0.5 \text{ m}$ .

### 3. EXPERIMENTAL RESULTS

#### (a) current start-up

In order to investigate how energetic electrons confined in the open configuration contribute to  $I_p^{\text{initial}}$ , three kinds of open configuration, whose  $R_{\text{mirror}}$  and the decay index  $n^*(=-d \ln B_z / d \ln R)$  are respectively, 0.85 and -0.02 at  $R=0.6 \text{ m}$  for the case (a), 1.2 and 0.2 for the case (b), and 2 and 0.5 for the case (c), are chosen.  $P_{\text{RF}}$  is 17 kW and the line density  $n_{e1}$  is  $< 1 \times 10^{17} \text{ m}^{-2}$ . The magnetic reconstruction using flux loop signals indicates that a closed magnetic surface is not formed for  $I_p^{\text{initial}}$  below 4 kA. Figure 1 shows the  $B_z$  dependence of  $I_p^{\text{initial}}$  and HXR flux ( $\Gamma_{\text{HX}}$ ) in the energy range of 10 – 60 keV. In the case (a), no current is observed for  $B_z < 0.8 \text{ mT}$ ,  $I_p^{\text{initial}}$  peaks at  $\sim 1 \text{ kA}$  at  $B_z \sim 1 - 1.2 \text{ mT}$  and decreases to zero for  $B_z > 1 \text{ mT}$ . The peak of  $\Gamma_{\text{HX}}$  ( $\sim 50$  counts/sec) also corresponds to the peak of  $I_p^{\text{initial}}$ , but no high energy ( $> 30 \text{ keV}$ ) HXR are observed (see Fig 1c). In the case (b), it is observed that  $I_p$  increases linearly up to 3.7 kA as  $B_z$  increases to 1.4 mT, and remains at  $1 \text{ kA} \pm 0.2 \text{ kA}$  for  $1.6 \text{ mT} < B_z < 2.8 \text{ mT}$ . At  $B_z = 1.4 \text{ mT}$   $\Gamma_{\text{HX}}$  shows the maximum, and at  $B_z = 1.6 \text{ mT}$  it is reduced and it is increased gradually again with increasing  $B_z$ . At the  $B_z > 1.6 \text{ mT}$ , the high energy component of HXR ( $> 30 \text{ keV}$ ) is increased. In the case (c)  $I_p^{\text{initial}}$  also

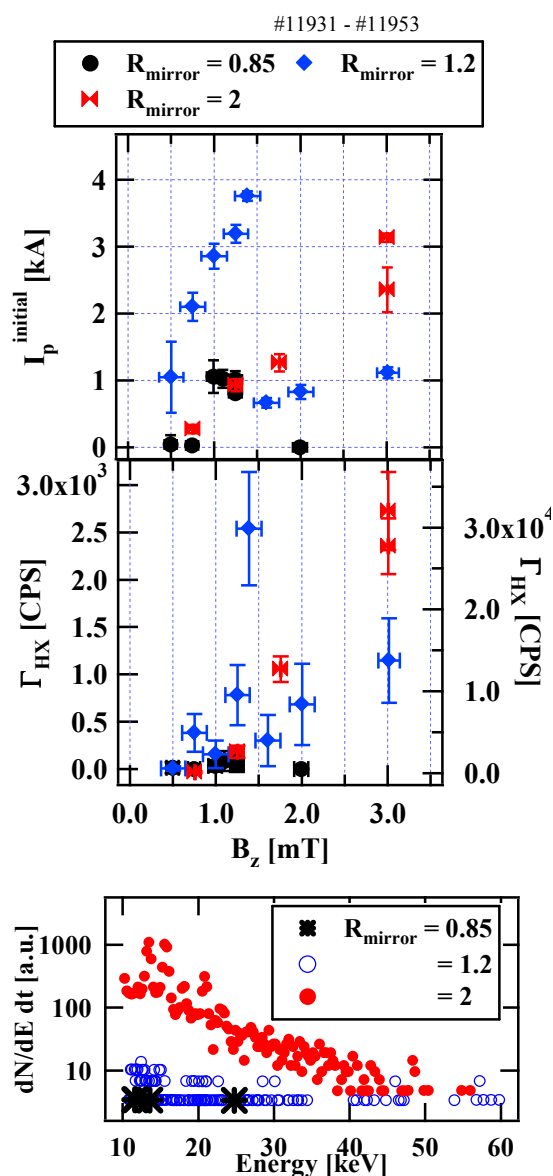


Figure 1 The  $B_z$  dependence of  $I_p$  and  $\Gamma_{\text{HX}}$  and energy spectra for  $R_{\text{mirror}} = 0.85, 1.2$  and 2 at  $B_z = 2 \text{ mT}$

increases up to 3 kA with a proportional constant which is a factor of three smaller than that in the case (b). No reduction in  $I_p^{\text{initial}}$  is observed. Although  $I_p^{\text{initial}}$  is  $< 3$  kA,  $\Gamma_{\text{HX}}$  is increased up to  $3 \times 10^4$  c/s at  $B_z = 3$  mT, which is one order of magnitude higher than that in the case (b). The energy spectrum shows that energetic electrons build up towards the higher energy range.

### (b) inboard poloidal field null configuration

Since the case (c) shows a favorable current start-up, current sustainment experiments have been performed under the condition of temporally constant  $B_z/B_t$  up to 10%.  $P_{\text{RF}}$  is 45 kW and  $n_e l$  is  $\sim 2 \times 10^{17} \text{ m}^{-2}$  ( $n_e < n_{\text{ecut}}$ ). Figure 2 shows the  $B_z$  dependence of  $I_p$ ,  $\Gamma_{\text{HX}}$  ( $> 50$  keV) and  $T_{\text{HX}}$ . Here,  $T_{\text{HX}}$  is determined from the slope of the energy spectrum. These three quantities increase with increasing  $B_z$  and are well kept constant in time. At  $B_z = 15$  mT  $I_p$  reaches up to 16 kA and the maximum energy extends to  $\sim 0.8$  MeV. If the number density of energetic electrons  $n_{\text{ehot}}$  is assumed  $0.1 n_e$  [9],  $\beta_{\text{pHX}} = n_{\text{ehot}} T_{\text{HX}} / (B_p^2 / 2\mu_0)$  can be evaluated, where  $B_p$  is the poloidal magnetic field.  $\beta_{\text{pHX}}$  is  $\sim 3.8$  and almost independent of  $B_z$ . Figure 3 shows the reconstructed magnetic flux with the inboard poloidal field null due to high  $\beta_p$ . These results indicate that in the case (c) electrons created by ECH can be well confined and accelerated with increasing  $B_z$ , and then as a result they contribute to formation and sustainment of the high  $\beta_p$  equilibrium.

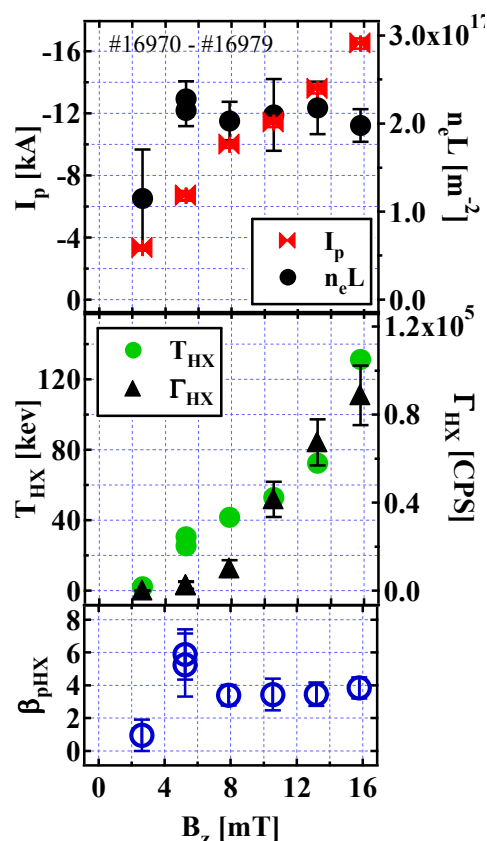


Figure 2 The  $B_z$  dependence of  $I_p$ ,  $n_e l$ ,  $T_{\text{HX}}$ ,  $\Gamma_{\text{HX}}$  and  $\beta_{\text{pHX}}$  in the case (c) ( $R_{\text{mirror}} = 2$ ).

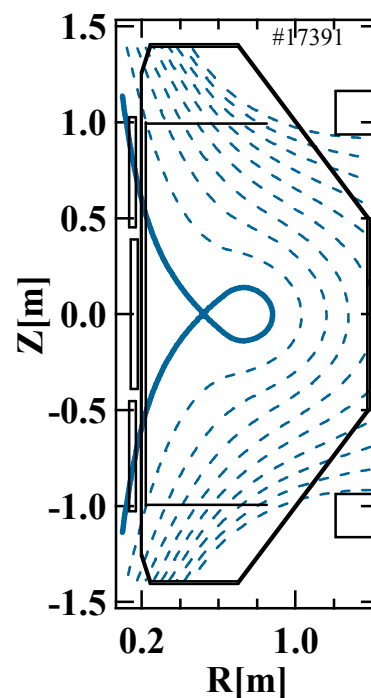


Figure 3 The magnetic flux contour of inner poloidal null configuration.

#### 4. Discussion and summary

The initial energy of electrons born near the cyclotron layer is evaluated at several keV [10], which can be supported by the fact that at the very beginning phase of the ECR, HXR  $\sim 10$  keV has been measured [11]. Since they are collisionless, a physical picture based on particle orbits is possible. In the case (a), since the curvature of the field lines is convex, co-moving electrons with stagnation orbits and mirror trapped particles with banana orbits cannot be confined. Thus the pressure-driven current might be a plausible mechanism. In cases (b) and (c) the contribution of  $j_{co}$  and  $j_{pr}$  to  $I_p^{initial}$  might be discriminated by orbit calculations taking the magnitude of  $B_z$  into account. The orbits of electron, having energy from 10 -30 keV, launched at  $R=0.6m$  and  $Z=0$  m show that when  $B_z$  is 1.2 mT co-moving electrons at 10 keV can be confined for the pitch angle( $\theta$ ) of  $> 60^\circ$  and at 30 keV for  $\theta > 0^\circ$ . Thus it is concluded that  $j_{co}$  contributes to  $I_p^{initial}$ . However, when  $B_z$  is 3 mT, they can be confined only for  $\theta \sim 85^\circ$ . This strong  $B_z$  dependence of stagnation orbits is ascribed to that the energy is proportional to  $B_z^2$ . On the other hand, the trapped particles for  $\theta > 65^\circ$  can be well confined. The width  $\Delta\theta$  of the trapped particles increases to  $45^\circ$  with for  $R_{mirror}=2$ . Therefore, it can be concluded that the trapped electrons dominate  $I_p^{initial}$  at high  $B_z$  and large  $R_{mirror}$ .

In the case of  $R_{mirror}=2$ , the inboard null configuration is found to be sustained in steady state. From the equilibrium relation  $B_z = \mu_0 I_p / 4\pi R ( \ln(8R/a) + l_i/2 - 3/2 + \beta_p )$  [12],  $\beta_p$  is evaluated as 3.87, which is consistent with  $\beta_{pHX}$ . Here,  $I_p = 11$  kA,  $B_z = 10$  mT,  $a = 0.15$ ,  $R = 0.73$  and  $l_i = 1.2$  are used. As shown in Fig. 2, since both  $\Gamma_{HX}$  and  $T_{HX}$  relate with  $B_z$  linearly, the hot pressure  $n_{ehot} T_{HX}$  is proportional to  $B_z^2$ . Thus, non-inductive current driven by EC waves leads to the high  $\beta_p$  equilibrium due to the better confinement of the energetic trapped particles.

#### References

- [1] C.B. Forest, et al., Phy. Rev. Lett. **68** (1992) 3559
- [2] C.B. Forest, et al., Phys. Plasmas **1** (1994) 1568
- [3] T. Maekawa, et al., Nucl. Fusion **45** (2005) 1439
- [4] A. Ejiri, et al., Nucl. Fusion **46** (2006) 709
- [5] V. Shevchenko, et al., Nucl. Fusion **50** (2010) 022004
- [6] L. E. Zakharov Sov, et al., J. Plasma Phys. **14** (1988) 75
- [7] Rome J.A, et al., Nucl. Fusion **19** (1979) 1293
- [8] T. Shimozuma, et al., Journal of the Physical Society of Japan **54** (1985) 1360
- [9] M. Ishiguro, et al., Review of Scientific Instruments **82** (2011) 113509
- [10] Peng Y-K.M, et al., Nucl. Fusion **18** (1978) 1489
- [11] S. Tashima, et al., Journal of Plasma and Fusion Research **9** (2010) 316
- [12] V. D. Shafranov, et al., Reviews of Plasma Physics Vol. 2, (Consultants Bureau, New York, 1966)